

Thermal detection of flux-flow noise in type-II superconductors

B. Plaçais and Y. Simon

Groupe de Physique des Solides de l'École Normale Supérieure, F-75231 Paris CEDEX 05, France

(Received 27 June 1988)

In this paper we present an original method for the observation of flux-flow noise. A superconducting slab, placed in a normal magnetic field, and immersed in He II, constitutes one of the walls of a rectangular second-sound resonator. As is well known, the voltage observed in the flux-flow regime is noisy, due to irregularities in the vortex motion. Therefore, noise in Joule dissipation is expected to occur, making the slab act as a noisy second-sound transmitter. Second-sound noise is then amplified selectively on the different modes of the resonator, with amplitudes depending, in general, on the spatial distribution and coherence of the fluctuating heat sources on the sample. Thus careful and detailed second-sound analysis should provide valuable information on vortex motion and pinning, that is not necessarily given by the usual voltage noise measurements. Preliminary experiments reported in this paper are merely intended to demonstrate that we are able to detect and identify the thermal flux-flow noise, in spite of its minuteness ($\sim 10^{-15}$ W²/Hz), while obtaining reliable quantitative results.

I. INTRODUCTION

Since the pioneering work of van Ooijen and van Gorp,^{1,2} flux-flow noise, associated with vortex motion in type-II superconductors, has been extensively studied, both theoretically³⁻⁵ and experimentally.⁶⁻⁹ It is one way of approaching the problem of vortex dynamics and pinning. (See, for instance, the review of Clem.¹⁰)

This noise appears, in the flux-flow regime, as a fluctuating component δV superposed on the dc voltage V . The existing theories are developments of the original idea of van Gorp and interpret $V + \delta V$ as the result of overlapping pulses due to individual vortices crossing over the sample, in a way quite similar to "shot noise" in electronics. In order to explain amplitudes and frequency shapes of the experimental power spectra, models require the introduction of many fitting parameters. van Gorp already introduced the "pinned vortex fraction" and the "flux bundle size" Φ .² In more recent papers, parameters describing statistical distributions of Φ and of transit and stopping times have been introduced.⁹ These *ad hoc* parameters make the models considerably more intricate while leaving fundamental difficulties unsolved. Often, constraints on the vortex dynamics are implied that hardly are reconcilable with the basic laws of conservation, namely vortex number and energy conservation. In contrast, we think that the two-dimensional description of the vortex motion in a slab normal to the magnetic field³ is an oversimplification, as it *a priori* excludes any variation of the current density distribution along the vortex lines. This assumption is at variance with recent experimental results,¹¹ as also with older ones,¹² revealing that a large part of the transport current flows near the surface of the sample. We believe that surface-to-volume fluctuations of the current density distribution might well be an important mechanism in noise generation. This point will be discussed in detail elsewhere. By fitting the experimental data, the authors infer the value of the flux

bundle size Φ ; it is found to be strongly decreasing with increasing applied current over several decades, from about $10^4 \phi_0$ down to the flux quantum ϕ_0 .² The limiting value ϕ_0 suggests that the flux-line lattice becomes amorphous at large current densities.² This conclusion is inconsistent with neutron diffraction experiments on a single crystal of vortex lines, where the observed effect of flux flow was, on the contrary, to improve the ordering of the vortices.¹³ All these difficulties led us to investigate another technique to observe flux-flow noise.

A noisy Joule effect $I\delta V$ is necessarily associated with the voltage noise δV . Therefore, if the sample is immersed in a superfluid helium bath, it behaves as a noisy second-sound source. Our purpose here is to show that it is possible to detect and analyze this second-sound noise, thanks to a technique of resonant amplification. The experimental principle is described in Sec. II. This method may appear as a very indirect and somewhat delicate way to retrieve δV . But, as explained in Sec. II, further second-sound analysis will provide extra information concerning localization and coherence of noise sources.

II. EXPERIMENTAL SETUP AND PROCEDURE

The superconducting sample we used is a $40 \times 6.9 \times 0.19$ mm³ slab, cold rolled from a Pb-10.5 wt. % In ingot (Ginzburg-Landau parameter $\kappa \approx 3.5$). The slab was glued on the $z=0$ wall of a second-sound resonator as shown in Fig. 1 and acts as a second-sound transmitter. The resonator is a parallelepipedic cavity $L \times w \times h = 55 \times 14 \times 17$ mm³. The cavity walls were machined from composite epoxy resin rods and carefully bonded with an epoxy adhesive.

In this experiment, we shall restrict ourselves to observe and analyze second sound in the neighborhood of the fundamental resonant mode in the z direction. The corresponding resonant frequency is $\omega_0 = \pi c_2 / h$, where c_2 is the temperature-dependent second-sound velocity

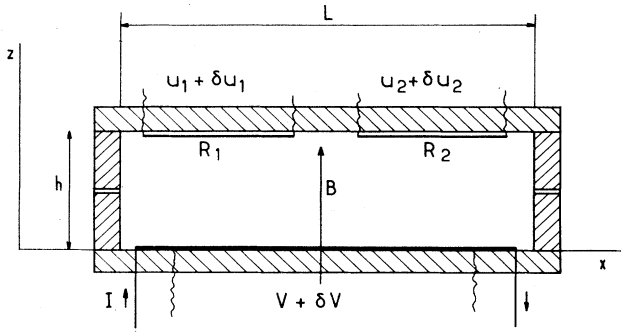


FIG. 1. Cross sectional sketch of the second-sound resonator. Internal dimensions of the cavity are $L \times l \times h = 55 \times 13 \times 17$ mm. A 0.5-mm-thick slit is made at the midheight of the cavity to allow the helium to flow inside, and the dc heat component to escape. The magnetic field B is applied perpendicular to the superconducting slab that is glued on the face $z=0$. Two carbon bolometers are painted on the face $z=h$.

($c_2 \leq 20$ m/sec). At the working temperature $T=1.75$ K, $\omega_0/2\pi=606$ Hz. Let $q_\omega(x,y)e^{i\omega t}$ be the ω component of the heat input, i.e., the inward-pointing normal component of the heat flux at a point (x,y) of the $z=0$ transmitting face. A classical calculation¹⁴ gives the temperature amplitude of the second-sound wave at the resonance as a function of the heat sources:

$$T_0(z) = \frac{Q_0 z_\infty}{\pi} q_0 \cos\left(\frac{\pi z}{h}\right). \quad (1)$$

Here Q_0 is the quality factor, characteristic of the mode ω_0 , defined as the ratio $\omega_0/\Delta\omega$ of the resonant frequency to the half-width $\Delta\omega$ of the common response curve (the usual convention in the second-sound literature). The best Q_0 obtained at 1.75 K was about 4500, which appears in second-sound acoustics as exceptionally good. z_∞ ($\sim 10^{-3}$ K cm²/W) is the thermal characteristic impedance of bulk superfluid helium. And q_0 is the average heat input over the transmitting wall $z=0$:

$$q_0 = \frac{1}{Lw} \iint q_\omega(x,y) dx dy. \quad (2)$$

At $\omega \sim 10^3$ sec⁻¹, the thermal skin depth of Pb-In (> 0.5 mm) is large enough compared with the sample thickness for any phase shift or attenuation due to thermal inertial effects to be neglected. On that condition, the sample may be regarded as a two-dimensional heat source. Thus $q_\omega(x,y)$ equals the ω component of the local dissipation on the sample, and zero elsewhere. By integrating on the sample surface, one obtains $q_0 = \delta P(\omega)/Lw$, where $\delta P(\omega)$ is the ω component of the total Joule effect VI . In the case of flux-flow noise, provided that the dc applied current is perfectly noise free, $\delta P(\omega) = I\delta V(\omega)$.

The temperature amplitude in the plane $z=h$ is measured independently by two carbon bolometers R_1 and R_2 ($R_1 \sim R_2 \sim 5$ k Ω). They were painted from a mixture of Aquadag and Indian ink. The addition of Indian ink

improves the bolometric sensitivity [$(1/R)dR/dT \sim 0.5$ K⁻¹ at 1.75 K].¹⁵ R_1 and R_2 are dc polarized with constant currents I_1 and I_2 (~ 1 mA) up to typical voltages $U_1 \sim U_2 \sim 5$ V. Let $H = \delta U/\delta P$ be the overall transfer function of the system cavity bolometer. H exhibits the resonant behavior of the cavity,

$$H = H_0 \left[1 + iQ_0 \frac{\omega - \omega_0}{\omega_0} \right]^{-1}, \quad (3)$$

and from the above data we expect $H_0 = H(\omega_0) \sim 0.1$ V/W (see Fig. 4).

One or two of the random signals δU_1 , δU_2 , and δV are preamplified and applied to the input channels of a digital spectrum analyzer (Solartron 1200). So any of the autopower or cross-power spectral densities such as S_{VV} , $S_{U_1 U_1}$, $S_{U_1 U_2}$, $S_{V U_1}$, etc. are available (see, for instance, Figs. 2 and 3). Due to the small amplitude of the flux-flow noise ($S_{VV} \sim 10^{-18}$ V²/Hz) δV is passed through a helium cooled step-up transformer (turns ratio 1:450) to overcome the preamplifier input noise ($\sim 10^{-16}$ V²/Hz).

We wish now to emphasize that a more detailed analysis of the second-sound response of the cavity should yield further information about the distribution of heat sources. It must be pointed out that the sources $q_\omega(x,y)$ in the geometry of Fig. 1 can also generate modes other than the longitudinal ones, even if with less efficiency. Let us consider, for example, the fundamental mode in the y direction,

$$T_1(y) = \frac{Q_1 z_\infty}{\pi} q_1 \cos\left(\frac{\pi y}{w}\right), \quad (4)$$

where now q_1 is a weighted average of $q_\omega(x,y)$ (see the Appendix in Ref. 16):

$$q_1 = \frac{1}{Lh} \iint q_\omega(x,y) \cos\left(\frac{\pi y}{w}\right) dx dy. \quad (5)$$

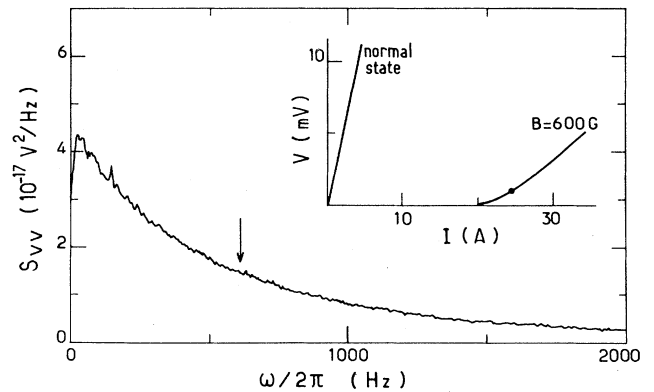


FIG. 2. Broadband recording of the power spectral density S_{VV} of the flux-flow voltage V . The voltage-current characteristic of the sample in the working conditions ($T=1.75$ K, $B=600$ G) is shown in the inset. The displayed S_{VV} corresponds to an applied dc current $I=24$ A ($V \approx 1$ mV); the arrow, at 606 Hz, marks the position of the fundamental mode of the second-sound resonator in the z direction (see Fig. 1).

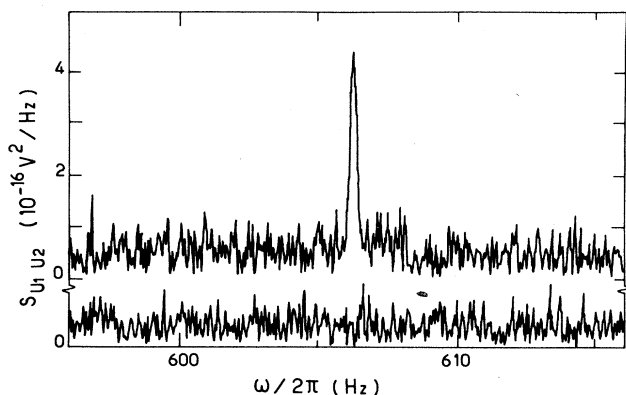


FIG. 3. The cross-power spectral density $S_{U_1 U_2}$ of the two bolometer voltages U_1 and U_2 . The upper curve shows the recording of the magnitude of $S_{U_1 U_2}$, about 606 Hz. For comparison, the lower curve shows another recording of $S_{U_1 U_2}$, in the normal state, at the same level of dissipation ($VI \approx 25$ mW).

From Eqs. (4) and (5) it is clear that q_1 will be zero, and the y mode will not be excited, if both amplitude and phase of $q_\omega(x, y)$ are independent of y ; this would be the case if the fluctuations of the vortex-line velocity were homogeneous and in phase all along the vortex path in the y direction across the sample. But in contrast, if we are concerned with flux jumps, incoherent at a small scale compared with the width of the sample, as suggested by the authors of Refs. 8 and 9, we must find $q_1 \sim q_0$. Thus in principle, an extensive study of the transverse modes amounts to performing a spatial Fourier analysis of the heat sources.

III. EXPERIMENTAL RESULTS

Figure 2 shows an example of the voltage power spectra $S_{VV}(\omega)$ we have observed on the Pb-In slab used in this experiment. Its amplitude and frequency shape are quite similar to those obtained by van Gurp *et al.*² However, in each experiment, one has to ascertain that a part of δV (if not all) is not due to spurious fluctuations of the state parameters. The magnetic field B , supplied by an electromagnet, exhibits fluctuations $\delta B \sim 1$ mG/Hz^{1/2} in the low-frequency range (0–10 Hz). To screen them, the cavity is placed inside a 1-cm-thick high-conductivity copper can. Moreover, we have verified the absence of any correlation between δV and δB , δB being measured with an external pick-up coil. On the other hand, we did not observe any appreciable voltage noise in the normal state; this corroborates the absence of significant noise δI in the applied current, which is supplied by 6 V–700 A h storage batteries.

Now we have to consider the role of fluctuations δT of the sample temperature. Indeed, since the critical currents are temperature dependent, any δT in the mixed state will make the cross voltage fluctuate, irrespective of the irregularities inherent to the vortex motion. In the conditions of Fig. 2, $(\partial V / \partial T)_{I, B} \sim 1$ mV/K, so that

$\delta T \sim 10^{-4}$ K in the typical 0–1000 Hz bandwidth (or $S_{TT} \sim 10^{-11}$ K²/Hz) could give rise to δV of the same order of magnitude as is observed. The fluctuations of the sample temperature may have various sources. Firstly we must exclude the influence of fluctuations of the bath temperature itself. It is to be noted that, even when using a temperature control system (classical bridge controller or second-sound controller¹⁶), any disturbance above a few Hz escapes regulation. But measurements of auto- and cross-power spectra of the bolometric signals δU_1 and δU_2 show that large-scale fluctuations of the bath temperature do not exceed $S_{TT} \sim 10^{-16}$ K²/Hz and consequently can be ignored. Even in a perfectly regulated bath, one can consider the local thermodynamic fluctuations of the sample temperature. As a matter of fact, according to Clarke and Voss, they are responsible for the $1/f$ noise in metallic films¹⁷ and in particular in tin and lead films at the superconducting transition.¹⁸ However these fluctuations are negligible in a bulk sample like the slab used here. Another possible source of δT noise could be changes in the thermal contact resistance between the dissipating sample and helium. This clearly occurs in the case of bubble generation in normal helium,^{2,8} and the resulting “flicker noise” overlaps the flux-flow noise. For this reason, authors usually prefer to work in superfluid helium. Yet there is between He II and a metal a strong thermal resistance, the Kapitza resistance ($R_K \sim 1$ K cm²/W). In the presence of a dc heat flux q , the sample temperature is raised to $R_K q$ degrees ($\sim 10^{-2}$ K) above the bath temperature. Thus δT fluctuations still could result from any fluctuation of R_K . Such δR_K , if they exist, would be analogous to the $1/f$ noise in resistors which is commonly interpreted in terms of resistance fluctuations. But this seems to be excluded by experiment for two reasons: No strong low-frequency component in the δV spectrum is observed, and δV tends to decrease while increasing the current in flux flow, at variance with the expected proportionality of δT with q .

To detect the thermal flux-flow noise, one could think of simply measuring the power spectral density S_{UU} of one bolometer, expecting here $S_{UU} = I^2 H^2 S_{VV}$, where H is the cavity-bolometer transfer function defined in Sec. II. But S_{UU} essentially consists of intrinsic bolometric noise, viz. the above mentioned $1/f$ noise; at low temperatures, Johnson noise is vanishingly small. We found $S_{UU} \approx U^2 C / f$ in accordance with Hooge’s law,¹⁹ where $C \sim 10^{-14}$ was the minimum value we were able to obtain by optimizing the bolometer dimensions. At $f \sim 1000$ Hz, the $1/f$ noise is still obscuring the expected thermal signal. That is the reason why two bolometers were fitted on the cavity. The measurement of the cross-power spectrum $S_{U_1 U_2}$ removes the incoherent $1/f$ noises. Figure 3 shows a recording of $S_{U_1 U_2}$ that reveals the thermal signal. The resonancelike shape of $S_{U_1 U_2}$, obtained after 2 h averaging, attests the thermal character of the signal, and excludes any spurious electrical influence which has no singularity in the displayed frequency range.

We have to prove that $S_{U_1 U_2}$ actually is associated with the flux-flow dissipation. Indeed, the resonant mode pos-

sibly could be excited by any spurious source, acting as a noisy heat input, such as bad current contacts on the sample, or local superfluid turbulence that makes the escape of the dc heat flux noisy (for instance, near accidental superfluid leaks). A first test consists in checking that an equivalent Joule power, occurring in the normal state, does not give rise to the same peak in $S_{U_1 U_2}$ (Fig. 3, lower). However, a decisive and quantitative test will be given by the measurement of the cross-power spectrum $S_{VU_1}(\omega)$. Again the intrinsic $1/f$ noise in R_1 will not contribute to S_{VU_1} that only involves that part of δU_1 correlated with δV . In the absence of any spurious capacitive influence between sample and bolometer, we expect that

$$\frac{S_{VU_1}}{S_{VV}} = \frac{\delta U_1(\text{thermal})}{\delta V} = \frac{H\delta P}{\delta V}, \quad (6)$$

where H is the thermal transfer function and δP the Joule source such as defined in Sec. II. Figure 4 shows two recordings of S_{VU_1}/S_{VV} . The upper part of Fig. 4 displays a calibration curve, obtained in the normal state by feeding a noisy current δI in the sample that is superimposed to the dc current. Thus, the slab acts as a noisy Joule source, with $\delta P = 2RI\delta I = 2I\delta V$, simulating the flux-flow noise, while otherwise retaining the same conditions of detection. By introduction of a scaling factor $2I$, the analyzer directly displays the thermal transfer function H , expressed in V/W . The recorded $H(\omega)$ has the expected frequency dependence according to Eq. (3). So we obtained at once the resonant frequency $\omega_0/2\pi = 606$ Hz, the quality factor $Q_0 = 4400$ and $H_0 = 0, 20$.

The lower part of Fig. 4 shows a recording of S_{VU_1}/S_{VV} in the same experimental conditions that in Fig. 4 (upper) and Figs. 3 and 2 ($T = 1.75$ K, $B = 600$ G, and $I = 24$ A). On subtracting the continuous background, the peak value at ω_0 is found to be equal to 4.8 ± 0.7 in good agreement with Eq. (6) and $H_0 = 0.20$, with $\delta P/\delta V = I = 24$ A.

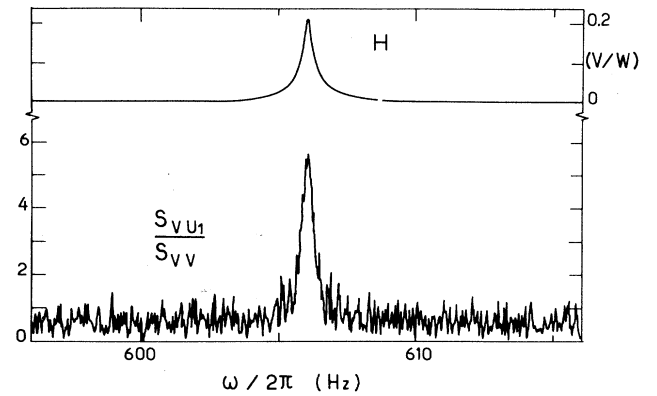


FIG. 4. The cross-power spectral density S_{VU_1} between the sample and the bolometer voltages, in normalized units. The upper curve shows the magnitude of $S_{VU_1}/2IS_{VV}$ such as obtained in the normal state with the purpose of calibration. It represents the modulus of the transfer function $H(\omega)$ of the system cavity bolometer, defined in the text. The lower curve is the dimensionless magnitude of the transfer function S_{VU_1}/S_{VV} , in the working conditions of Fig. 2, obtained after averaging over a period of 2 h.

IV. CONCLUSIONS

We have shown that, thanks to a second-sound amplification technique, it is possible to detect the thermal noise associated with flux-flow noise and to obtain reliable quantitative results. In some respects, thermal noise measurements are, for the present, nothing but an indirect measurement of the voltage noise δV , since the bolometric signal, denoted as $H\delta P$ in the text, is directly proportional to δV . However, as shown in Sec. II, the investigation of the transverse modes of a second-sound resonator can yield additional data and not merely the mean Joule dissipation $\delta P = I\delta V$. In this manner, we hope to gain new information about the spatial distribution of dissipation and, thereby, shed some light on the problems of erratic vortex motion and pinning.

¹D. J. Van Ooijen and G. J. Van Gorp, Phys. Lett. **17**, 230 (1965).

²G. J. van Gorp, Phys. Rev. **166**, 436 (1968).

³J. R. Clem, Phys. Rev. B **1**, 2140 (1970).

⁴R. E. Burgess, Physica **55**, 369 (1971).

⁵J. G. Park, J. Phys. F **2**, 957 (1972).

⁶S. W. Shen and A. van der Ziel, Physica **64**, 587 (1973).

⁷P. Jarvis and J. G. Park, J. Phys. F **5**, 1573 (1975).

⁸C. Heiden, D. Kohake, W. Krings, and L. Ratke, J. Low Temp. Phys. **27**, 1 (1977).

⁹J. Thompson and W. C. H. Joiner, Phys. Rev. B **20**, 91 (1979).

¹⁰J. R. Clem, Phys. Rep. **75**, 1 (1981).

¹¹P. Mathieu and Y. Simon, Europhys. Lett. **5**, 67 (1988).

¹²P. Thorel, Y. Simon, and A. Guetta, J. Low Temp. Phys. **11**,

333 (1973).

¹³P. Thorel, R. Kahn, Y. Simon, and D. Cribier, J. Phys. **34**, 447 (1973).

¹⁴P. Mathieu, J. C. Marechal, and Y. Simon, Phys. Rev. B **22**, 4293 (1980).

¹⁵K. Noto, N. Kobayashi, and Y. Muto, Jpn. J. Appl. Phys. **15**, 2449 (1976).

¹⁶P. Mathieu, A. Serra, and Y. Simon, Phys. Rev. B **14**, 3753 (1976).

¹⁷J. Clarke and R. F. Voss, Phys. Rev. Lett. **33**, 24 (1974).

¹⁸J. Clarke and R. F. Voss, Phys. Rev. Lett. **34**, 1217 (1975).

¹⁹F. N. Hooge and A. M. H. Hoppenbrouwers, Physics **45**, 386 (1969).